ChemComm

RSCPublishing

COMMUNICATION

# Graphene-supported ferric porphyrin as a peroxidase mimic for electrochemical DNA biosensing†

Cite this: *Chem. Commun.*, 2013, **49**, 916

Received 21st October 2012, Accepted 6th December 2012

DOI: 10.1039/c2cc37664d

www.rsc.org/chemcomm

Quanbo Wang, Jianping Lei,* Shengyuan Deng, Lei Zhang and Huangxian Ju*

**A novel peroxidase mimic was designed by loading ferric porphyrin and streptavidin onto graphene, which was used to recognize a biotinylated molecular beacon for specific electrochemical detection of DNA down to attomolar levels.**

Horseradish peroxidase (HRP) has been extensively used in analytical fields primarily due to its excellent capacity for catalysis. It can be used as a trace label to increase the detectability of target analytes by different detection protocols from traditional enzyme-linked immunosorbent assays to newly developed immunosensors,[1] DNA sensors,[2] aptasensors[3] and cytosensors.[4] Besides, loading HRP onto various nanomaterials has become a promising way to further amplify the detection signal and achieve a lower detection limit for the analyte.[5] However, the relative large protein structure of HRP limits its maximum loading amount, which is adverse to signal amplification. Furthermore, as a natural enzyme, its activity is highly dependent on protein conformation, leading to vulnerability to external conditions.[6a] Thus, the mimicking of HRP is of great importance and remains a challenging topic.[6]

Since the catalytic centre of HRP is actually an iron-containing porphyrin complex, mimicking the biological function of HRP using iron porphyrins such as hemin and iron(III) meso-tetrakis(*N*-methylpyridinum-4-yl)porphyrin (FeTMPyP) has attracted considerable interest.[7] However, free ferric porphyrins in aqueous solution usually show much weaker peroxidase activity than HRP, which can be attributed to the oxidative destruction and the self-aggregation of ferric porphyrin molecules to form catalytically inactive species.[7b] In order to achieve good catalytic performance, the key point in the design of HRP mimicking analogues is to choose a suitable carrier for loading the ferric porphyrin molecules and maintaining their intrinsic peroxidase activity. G-quadruplex DNA oligomers have been considered as a successful carrier for hemin,[7a,8] and graphene has also been used as a carrier of porphyrins for the preparation of electrochemical[9] or optical[10] sensors. Very recently, a graphene-supported hemin complex with enhanced catalytic activity for the oxidization of pyrogallol has been designed.[7b] This work demonstrates the design of a novel HRP mimic with high peroxidase activity and the first use of the porphyrin-based mimic as a trace label for biosensing.

The mimic was prepared by assembling ferric porphyrin on graphene *via* π–π stacking and labelled with streptavidin by an amidation reaction. The obtained trace label showed greatly enhanced peroxidase activity toward *o*-phenylenediamine (*o*-PD) oxidization in the presence of $H_2O_2$, leading to improved sensitivity for electrochemical biosensing. By combining it with a biotinylated molecular beacon (MB), a sensitive DNA biosensing method was thus developed (Scheme 1).

The DNA biosensor was prepared by immobilizing the biotinylated MB on a gold nanoparticles-single-walled carbon nanohorn (AuNPs–SWCNH) composite modified glassy carbon

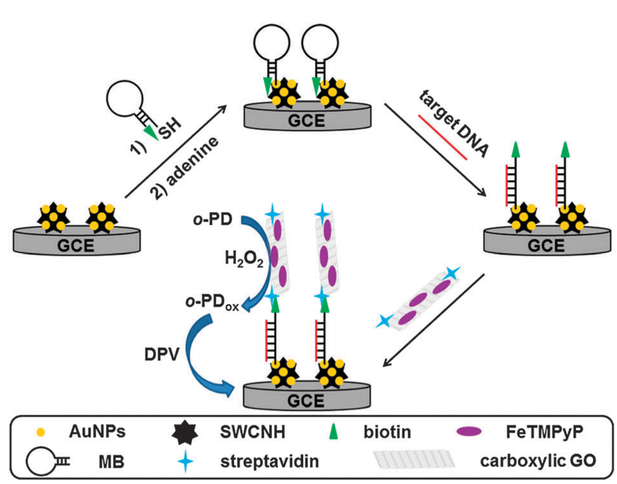


**Scheme 1** Schematic illustration of graphene-supported ferric porphyrin as a HRP mimicking trace label for electrochemical detection of DNA.

*State Key Laboratory of Analytical Chemistry for Life Science, School of Chemistry and Chemical Engineering, Nanjing University, Nanjing 210093, P.R. China. E-mail: hxju@nju.edu.cn*

† Electronic supplementary information (ESI) available: Experimental details and additional figures. See DOI: 10.1039/c2cc37664d



This journal is © The Royal Society of Chemistry 2013

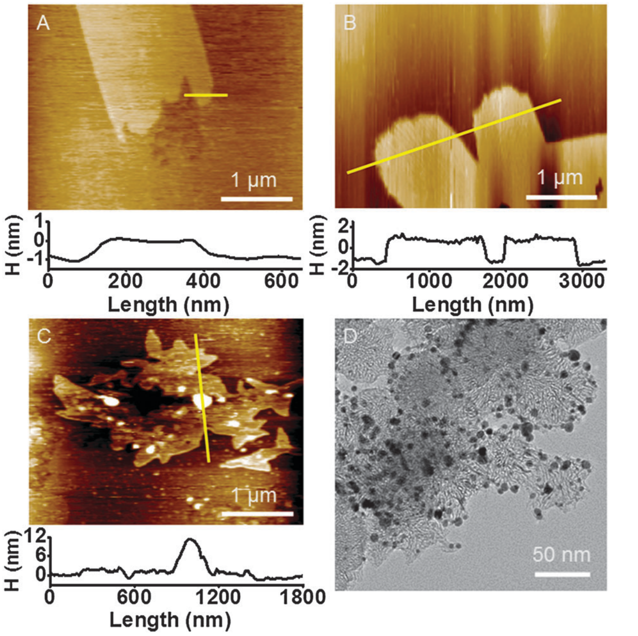


**Fig. 1** AFM images of (A) carboxylic GO, (B) FeTMPyP–GO and (C) FeTMPyP–streptavidin–GO bioconjugate, and (D) TEM of AuNPs–SWCNH composite.

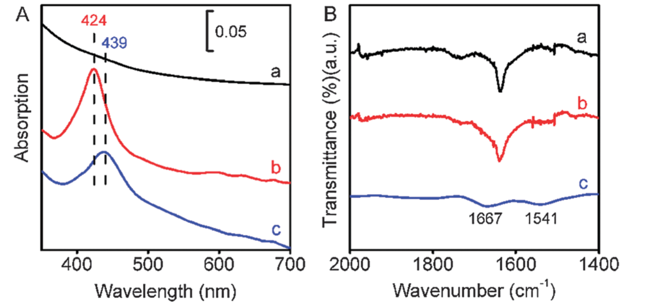


**Fig. 2** (A) UV-vis spectra of (a) carboxylic GO, (b) FeTMPyP and (c) FeTMPyP–streptavidin–GO bioconjugate. (B) FTIR spectra of (a) FeTMPyP–GO, (b) FeTMPyP–streptavidin–GO bioconjugate, and (c) their difference.

electrode (ESI†). In the absence of target DNA, the MB probe was expected to be in the ''closed'' state, thus the streptavidin on the trace label was blocked from the specific interaction with the shielded biotin due to the large steric effect. Contrarily, after the MB probe hybridized with target DNA, the resulting rigid duplex structure was expected to move the biotin group away from the electrode surface, making the biotin end easily accessible to the trace label. Thus a ''signal on'' electrochemical biosensor based on a porphyrin-based HRP mimic as a trace label was developed for the highly sensitive and specific detection of target DNA.

Carboxylic graphene oxide (GO) was chosen as carrier for preparation of the porphyrin-based mimic. Tapping mode atomic force microscopy (AFM) was used to determine the thickness of the GO during the bioconjugate fabrication. The original carboxylic GO showed a thickness of 0.8 nm (Fig. 1A), corresponding to its single-layer nature. After non-covalent assembly of FeTMPyP, its thickness increased to about 2.0 nm (Fig. 1B). Considering that the thickness of one porphyrin molecule is about 0.5 nm, the thickness increase can be attributed to the assembly of monolayer FeTMPyP on the both sides of the GO. Compared with the relatively smooth surface of FeTMPyP–GO, the surface of the FeTMPyP–streptavidin–GO bioconjugate is rough (Fig. 1C), while the thickness at the position of the bound protein increased to around 10 nm, indicating the successful loading of streptavidin onto the surface of FeTMPyP–GO.

The transmission electron micrograph (TEM) of the AuNPs–SWCNH composite clearly demonstrated that AuNPs of 5–8 nm diameter were deposited on the surface of the SWCNHs (Fig. 1D), which accelerated the electron transfer for the construction of a highly sensitive electrochemical sensing platform.

The FeTMPyP–streptavidin–GO bioconjugate was characterized using UV-vis spectroscopy (Fig. 2A). The carboxylic GO did not display an obvious absorption peak (curve a), while FeTMPyP featured an intense Soret band at 424 nm together with three weak Q bands at longer wavelengths (curve b). After assembly on the GO surface, the Soret band of FeTMPyP showed a 15 nm red-shift due to the molecular flattening of FeTMPyP during the assembly process[10a] (curve c). This indicated a strong interaction between GO and the FeTMPyP molecules, which is helpful in preventing the leakage of FeTMPyP and maintaining the catalytic activity of the FeTMPyP–streptavidin–GO bioconjugate.

Fourier transformation infrared (FTIR) spectroscopy was also used to characterize the FeTMPyP–streptavidin–GO bioconjugate (Fig. 2B). In comparison with the FTIR spectrum of FeTMPyP–GO (curve a), the FTIR spectrum of FeTMPyP–streptavidin–GO bioconjugate displayed obvious absorption peaks corresponding to the amide bands I (1667 $cm^{-1}$) and II (1541 $cm^{-1}$) of streptavidin, respectively (curves b and c), which indicated that the streptavidin was successfully linked on the bioconjugate by amidation reaction.

The peroxidase activity of the FeTMPyP–streptavidin–GO bioconjugate was tested by differential pulse voltammetric (DPV) measurements in PBS containing 10 mM *o*-PD and 8.0 mM $H_2O_2$. The FeTMPyP–streptavidin–GO modified glassy carbon electrode (GCE) exhibited a stable DPV peak at $-0.524$ V with a peak current of $-2.21$ μA (Fig. S1, ESI,† curve a), which corresponded to the reduction of 2,2′-diaminoazobenzene (*o*-$PD_{ox}$), the oxidation product of *o*-PD by $H_2O_2$ catalysed by FeTMPyP–streptavidin–GO bioconjugate.[4] Contrarily, the FeTMPyP modified GCE showed a very weak DPV peak of only $-0.10$ μA (Fig. S1, ESI,† curve b), which was 22.1 times lower than that of the FeTMPyP–streptavidin–GO modified GCE, suggesting that the peroxidase activity came from the integration of GO and FeTMPyP, which is consistent with a previous report.[7b]

The assembly of the AuNPs–SWCNH on the GCE led to an increase in background current, while the following MB, target DNA and FeTMPyP–streptavidin–GO assemblies did not change the background (Fig. S2, ESI†). The FeTMPyP–streptavidin–GO/target DNA/MB/AuNPs–SWCNH/GCE showed a rough surface (Fig. S3, ESI†). Upon addition of *o*-PD by $H_2O_2$, the cyclic voltammogram showed a couple of well-defined redox peaks

This journal is © The Royal Society of Chemistry 2013 

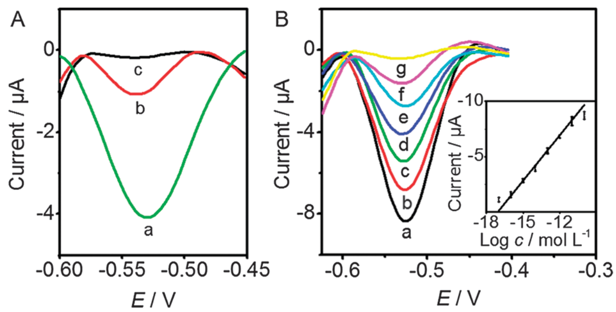


**Fig. 3** (A) DPV responses with (a) FeTMPyP–streptavidin–GO and (b) HRP–streptavidin–GO as trace label and (c) without trace label at 10 fM target DNA. (B) DPV curves at (a) 10, (b) 1 pM, (c) 100, (d) 10, (e) 1.0 fM, (f) 100 and (g) 0 aM target DNA. Inset: plot of peak current *vs.* the logarithm of target DNA concentration.

at −0.455 and −0.606 V (Fig. S2, ESI†). At the target DNA concentration of 10 fM, the peak current of DPV was −3.92 μA (Fig. 3A, curve a), which was 3.56 times larger than −1.10 μA obtained with the HRP–streptavidin–GO bioconjugate as trace label (Fig. 3A, curve b). The high DPV response of the FeTMPyP–streptavidin–GO bioconjugate highlighted the much smaller molecular dimension of FeTMPyP for higher loading, which afforded abundant peroxidase catalytic sites for the oxidization of *o*-PD. In addition, in the absence of a trace label, the modified GCE exhibited a negligible DPV peak (Fig. 3A, curve c).

The electrochemical response of the proposed DNA biosensor was affected by the incubation time of trace label. With increasing incubation time, the DPV response increased and reached a plateau at 30 min (Fig. S4, ESI†). Therefore, 30 min was chosen as the optimal incubation time, at which the DPV signal increased with the increasing target DNA concentration (Fig. 3B). The plot of the DPV peak current *vs.* the logarithmic value of the target concentration showed a linear relationship over 5 orders of magnitude from 10 pM to 100 aM. In the absence of target DNA, the DPV curve showed a much smaller response than the DPV peak at 100 aM (Fig. 3B, curve g), which was probably a result of the nonspecific adsorption of the enzyme mimic on the GCE surface. The detection limit was calculated to be 22 aM at 3$\sigma$, which corresponded to 0.13 zmol in 6 μL solution. This improved analytical performance can be ascribed to the high loading of FeTMPyP and the unique structure with the cone-shaped tips of the SWCNHs.

The biosensor exhibited high specificity (Fig. S5, ESI†) and excellent anti-interference ability (Fig. S6, ESI†). The responses of five freshly fabricated biosensors to 10 fM DNA showed a relative standard deviation of 5.1%, indicating good fabrication reproducibility.

This work demonstrated a simple and convenient pathway to fabricate a universal peroxidase mimic by loading FeTMPyP onto carboxylic GO. The noncovalent π–π interaction led to a stable monolayer stacking of FeTMPyP on both sides of the GO, which produced a high loading of small FeTMPyP molecules. The integration of GO and FeTMPyP endowed the FeTMPyP with high peroxidase activity. Using the porphyrin-based mimic as a trace label, a method for specific detection of DNA was proposed by combining it with a biotinylated MB immobilized on a AuNPs–SWCNH modified electrode. This method showed a detection limit down to attomolar levels, much lower than that obtained with a HRP-based trace label. The biosensing method could discriminate target DNA from single-base or three-base mismatched oligonucleotides. The porphyrin-based trace label provides a novel alternative to natural enzymes for signal amplification, and could be easily extended to detect other analytes.

This research was financially supported by the National Basic Research Program of China (2010CB732400), and the National Natural Science Foundation of China (21075060, 21121091).

## Notes and references

1 (*a*) A.-M. J. Haque, H. Park, D. Sung, S. Jon, S.-Y. Choi and K. Kim, *Anal. Chem.*, 2012, **84**, 1871–1878; (*b*) G. X. Qin, S. L. Zhao, Y. Huang, J. Jiang and F. G. Ye, *Anal. Chem.*, 2012, **84**, 2708–2712.
2 G. Liu, Y. Wan, V. Gau, J. Zhang, L. H. Wang, S. P. Song and C. H. Fan, *J. Am. Chem. Soc.*, 2008, **130**, 6820–6825.
3 Y. L. Wen, H. Pei, Y. Wan, Y. Su, Q. Huang, S. P. Song and C. H. Fan, *Anal. Chem.*, 2011, **83**, 7418–7423.
4 W. Cheng, L. Ding, S. J. Ding, Y. B. Yin and H. X. Ju, *Angew. Chem., Int. Ed.*, 2009, **48**, 6465–6468.
5 (*a*) W. W. Zhao, X. Y. Dong, J. Wang, F. Y. Kong, J. J. Xu and H. Y. Chen, *Chem. Commun.*, 2012, **48**, 5253–5255; (*b*) D. Du, L. M. Wang, Y. Y. Shao, J. Wang, M. H. Engelhard and Y. H. Lin, *Anal. Chem.*, 2011, **83**, 746–752; (*c*) R. Malhotra, V. Patel, J. P. Vaqué, J. S. Gutkind and J. F. Rusling, *Anal. Chem.*, 2010, **82**, 3118–3123; (*d*) S. Y. Niu, Y. Jiang and S. S. Zhang, *Chem. Commun.*, 2010, **46**, 3089–3091.
6 (*a*) Y. J. Song, K. G. Qu, C. Zhao, J. S. Ren and X. G. Qu, *Adv. Mater.*, 2010, **22**, 2206–2210; (*b*) L. Z. Gao, J. Zhuang, L. Nie, J. B. Zhang, Y. Zhang, N. Gu, T. H. Wang, J. Feng, D. L. Yang, S. Perrett and X. Y. Yan, *Nat. Nanotechnol.*, 2007, **2**, 577–583; (*c*) H. Wei and E. K. Wang, *Anal. Chem.*, 2008, **80**, 2250–2254.
7 (*a*) P. Travascio, Y. F. Li and D. Sen, *Chem. Biol.*, 1998, **5**, 505–517; (*b*) T. Xue, S. Jiang, Y. Q. Qu, Q. Su, R. Cheng, S. Dubin, C.-Y. Chiu, R. Kaner, Y. Huang and X. F. Duan, *Angew. Chem., Int. Ed.*, 2012, **51**, 3822–3825; (*c*) Q. G. Wang, Z. M. Yang, X. Q. Zhang, X. D. Xiao, C. K. Chang and B. Xu, *Angew. Chem., Int. Ed.*, 2007, **46**, 4285–4289; (*d*) H. Yamaguchi, K. Tsubouchi, K. Kawaguchi, E. Horita and A. Harada, *Chem.–Eur. J.*, 2004, **10**, 6179–6186.
8 (*a*) D. Li, A. Wieckowska and I. Willner, *Angew. Chem., Int. Ed.*, 2008, **47**, 3927–3931; (*b*) S. Shimron, F. Wang, R. Orbach and I. Willner, *Anal. Chem.*, 2012, **84**, 1042–1048; (*c*) L. H. Tang, Y. Liu, M. M. Ali, D. K. Kang, W. A. Zhao and J. H. Li, *Anal. Chem.*, 2012, **84**, 4711–4717; (*d*) A. X. Zheng, J. Li, J. R. Wang, X. R. Song, G. N. Chen and H. H. Yang, *Chem. Commun.*, 2012, **48**, 3112–3114; (*e*) S. Bi, L. Li and Y. Y. Cui, *Chem. Commun.*, 2012, **48**, 1018–1020; (*f*) X. Zhu, X. Y. Gao, Q. D. Liu, Z. Y. Lin, B. Qiu and G. N. Chen, *Chem. Commun.*, 2011, **47**, 7437–7439.
9 (*a*) L. Y. Feng, L. Wu, J. S. Wang, J. S. Ren, D. Miyoshi, N. Sugimoto and X. G. Qu, *Adv. Mater.*, 2012, **24**, 125–131; (*b*) W. W. Tu, J. P. Lei, S. Y. Zhang and H. X. Ju, *Chem.–Eur. J.*, 2010, **16**, 10771–10777.
10 (*a*) Y. X. Xu, L. Zhao, H. Bai, W. J. Hong, C. Li and G. Q. Shi, *J. Am. Chem. Soc.*, 2009, **131**, 13490–13497; (*b*) Y. J. Guo, L. Deng, J. Li, S. J. Guo, E. K. Wang and S. J. Dong, *ACS Nano*, 2011, **5**, 1282–1290.


This journal is © The Royal Society of Chemistry 2013